UNCLASSIFIED

AD NUMBER
AD332122
CLASSIFICATION CHANGES
TO: unclassified
FROM: confidential
LIMITATION CHANGES
TO: Approved for public release, distribution unlimited
FROM: Distribution authorized to U.S. Gov't. agencies and their contractors; Administrative/Operational Use; 01 JUN 1962. Other requests shall be referred to Naval Ordnance Lab., White Oak, MD.
AUTHORITY
USNSWC ltr, 4 Dec 1974; USNSWC ltr, 4 Dec 1974

THIS PAGE IS UNCLASSIFIED

UNCLASSIFIED

AD 332 122

Reproduced
by the

ARMED SERVICES TECHNICAL INFORMATION AGENCY
ARLINGTON HALL STATION
ARLINGTON 12, VIRGINIA

UNCLASSIFIED

NOTICE: When government or other drawings, specifications or other data are used for any purpose other than in connection with a definitely related government procurement operation, the U. S. Government thereby incurs no responsibility, nor any obligation whatsoever; and the fact that the Government may have formulated, furnished, or in any way supplied the said drawings, specifications, or other data is not to be regarded by implication or otherwise as in any manner licensing the holder or any other person or corporation, or conveying any rights or permission to manufacture, use or sell any patented invention that may in any way be related thereto.

[redacted]

NOLTR 62-96

332122

332122

CATALOGED BY ASTIA
AS AD No.

UNDERWATER EXPLOSIONS BENEATH ICE (U)

RELEASED TO ASTIA
BY THE NAVAL ORDNANCE LABORATORY
☑ Without restrictions
☐ For Release to Military and Government Agencies Only.
☐ Approval by BuWeps required for release to contractors.
☐ Approval by BuWeps required for all subsequent release.

NOL

UNITED STATES NAVAL ORDNANCE LABORATORY, WHITE OAK, MARYLAND

1 JUNE 1962

ASTIA
OCT 19 1962

NOTICE: This material contains information affecting the national defense of the United States within the meaning of the Espionage Laws, Title 18, U.S.C. Sections 793 and 794, the transmission or revelation of which in any manner to an unauthorized person is prohibited by law.

NOLTR 62-96

NOX

[redacted]

Downgraded at 3 Year Intervals
Declassified after 12 Years. DOD Dir 5200.10

UNDERWATER EXPLOSIONS BENEATH ICE (U)

by

Robert M. Barash

Approved by: E. Swift, Jr., Chief
Underwater Explosions Division

ABSTRACT: The effects of underwater explosions beneath lake ice and Arctic ice have been studied experimentally. The results are applicable to the prediction of underwater damage ranges from nuclear bursts beneath ice, and to the design of an explosive ice destructor to provide nuclear submarines with quick access to the surface.

The underwater shock wave pressure history is described as the superposition of arrivals via five types of propagation path. The order of arrivals and the pressure contributions vary considerably as a function of the geometry.

For the ice-breaking application, an explosive with high bubble energy is recommended, since the resultant hole radius is shown to be proportional to the free-water maximum bubble radius, for a given type of ice.

EXPLOSIONS RESEARCH DEPARTMENT
U. S. NAVAL ORDNANCE LABORATORY
WHITE OAK, SILVER SPRING, MARYLAND

NOLTR 62-96 1 June 1962

Underwater Explosions Beneath Ice (U)

This report is a transcript of an oral presentation given at the Sixth Navy Science Symposium on 3 May 1962. It presents a summary of some preliminary experimental findings related to two problems of significance in the use of the Arctic Ocean as an operational area for nuclear submarines.

The study of explosion shock wave propagation under ice was performed under WEPTASK No. RE01-ZA732/212-9/WF008-21-003, Delivery Criteria for Underwater Nuclear Weapons and the work on explosive ice breaking was done under WEPTASK No. RUME-3-E-000/212-1/WF008-10-004 PA 002, Supporting Research in Underwater Explosives and Explosions. Some of the work on the latter subject was done under WEPTASK No. RUME-2-E-000/212-1/WF008-01-007 PA 031, Advanced Mines Supporting Research: Applied Research Analysis and Planning, and WEPTASK No. RUME-2-Q-000/212-1/WF008-20-002 PA 107, Explosive Destructor EX-27 and is also reported in NOLTR 61-146.

W. D. COLEMAN
Captain, USN
Commander

C. J. Aronson

C. J. ARONSON
By direction

CONTENTS

ILLUSTRATIONS

UNDERWATER EXPLOSIONS BENEATH ICE (U)

I. INTRODUCTION

With growing interest in the use of the Arctic Ocean as an operational area for submarines, some questions are being raised about the effects of underwater explosions beneath Arctic ice.

One such question concerns the damage inflicted upon an underwater target by the shock wave from an underwater explosion. Theoretical and experimental studies have been made of how the amplitudes and shapes of underwater shock wave pressure pulses can be modified by the presence of the ocean surface and of the ocean bottom (References (a) to (k))*. We are now interested in knowing what happens when the free surface of the ocean is replaced by a layer of ice.

Another question related to Arctic operations concerns the use of high explosives to break a clearing in the ice pack, so that nuclear submarines traveling under thick ice can have quick access to the surface.

As an early step in exploring these and several other questions experimentally, a test series was conducted at a freshwater lake in Minnesota called Moonshine Lake. The ice was about two feet thick. More than 40 TNT spheres were fired, ranging in weight from one pound to about 40 pounds. The charge position varied from 20 feet below the ice to 2 feet above the ice. Some preliminary results of these tests will be presented here.

II. UNDERWATER SHOCK WAVE PRESSURES

Underwater shock wave pressures at Moonshine Lake were measured with 1/4-inch diameter tourmaline crystal gages. The pressure sensed by each gage was displayed as a vertical deflection on an oscilloscope and recorded on a rotating drum camera to produce the pressure-vs-time records presented here.

A. PROPAGATION PATHS

The pressure history at a particular underwater gage location can be described, in general, as the superposition of several arrivals of the shock wave pulse, over different paths, with different arrival times.

Figure 1 shows four possible propagation paths - ray paths - from a particular explosion location to one particular

*Such letters refer to list of references on Page 10.

gage location. By means of arrival time calculations, these four paths have been shown to correspond to various events on the pressure-vs-time records from the underwater gages at Moonshine Lake.

One path is the direct shock wave path. Another is the reflection path, in which the shock wave is reflected from the bottom of the ice. A third path is the one corresponding to what is designated here as the "ice" wave. The fourth path illustrated here is the air reflection path.

The experimental results can perhaps be described most clearly by first considering each type of arrival separately, and looking at the corresponding portions of some pressure records.

B. PRESSURE RECORDS FOR EACH TYPE OF ARRIVAL

1. Direct Shock Wave. Figure 2 shows a pressure-vs-time record of a direct shock wave. This pressure pulse is typical of underwater explosion shock wave pulses in free water - that is, homogeneous water with no nearby boundaries. There is a sudden rise in pressure, followed by a decay which is exponential at first, and slower at later times.

2. Reflected Wave. Figure 3 shows portions of four different pressure-time records - only those portions in which the reflected wave appears. In all cases the reflected wave is superposed on the tail of the direct shock wave, because its path length is greater than that of the direct shock wave. The four records illustrate qualitatively the variations in the reflected wave as a function of the angle of incidence.

Record (a) represents a configuration in which the angle of incidence, α , is small - that is, the ray direction is close to the normal. The shape of the reflected pulse is similar to that of the direct shock wave pulse, but the amplitude is lower, partly because of the greater path length, and partly because only a fraction of the incident energy is reflected from the interface.

The other three records represent angles of incidence greater than the critical angle - that is, the angle beyond which all the energy is reflected and none transmitted, considering only compressional waves. In record (b), the pressure in the reflected wave decays quickly. The pressure contribution from the reflected wave then goes negative, bringing the resultant pressure to a lower value than that due to the direct wave alone.

As the incident angle is increased further, represented by record (c), the initial positive pressure contribution of the reflected wave is weaker, and has a gradual rise, rather than a sharp front. The decay is very fast.

In record (d), the positive portion of the pulse has virtually vanished, and the fast decay has become virtually a negative step.

In each of the last three records, the pulse shape appears to be distorted in the manner that would be expected if the incident pulse had undergone a phase shift independent of frequency. The variation among the four records is qualitatively in agreement with the prediction of acoustic theory that the phase shift of a reflected wave varies from 0^{o} to 180^{o} as the angle of incidence varies from the critical angle to glancing. (See (i) and (k).)

Acoustic theory, however, is inadequate in describing most of the reflected wave data. This is demonstrated by the two pressure-time curves in Figure 4. In both cases the charge weight was the same. The path length was the same, and the angle of incidence was the same, at least as far as these two can be determined simply from the geometry. The only difference is that the positions of the charge and gage are interchanged, so that in case (a) the peak pressure incident on the interface is about 2000 psi, while in case (b) the incident pressure is about 8000 psi. Acoustic theory alone - that is, the theory of low amplitude waves - does not predict any difference between the two results, and is therefore inadequate. Instead, a finite amplitude theory is required - one that takes into account the magnitude of the incident pressure.

Previous analyses (j) indicate how the non-linear effects arise. The reflected wave front propagates into a region through which the incident wave front has just passed. In the case of acoustic waves, the incident wave front leaves behind it a region which is in approximately the same state as the undisturbed medium. In the case of finite amplitude waves, however, the incident wave front leaves behind it a region of high density and appreciable particle velocity; and it is into this region that the reflected wave must propagate. As a result, the angle of reflection is not, in general, equal to the angle of incidence, and the ratio of reflected pressure to incident pressure is different from that for the acoustic case. For sufficiently high values of incident angle and incident pressure, the reflection configuration breaks down qualitatively also.

Figure 5 describes empirically the reflection factor as a function of the incident angle, α , for five different values of incident pressure. The reflection factor is defined here in a special way. It is the ratio of the peak pressure contribution of the reflected wave, measured at a particular gage location, to the pressure that would be expected there if the pulse underwent no loss in peak pressure upon reflection. Both α and the reflection factor were determined using the assumption of an acoustic reflection path, which is a simple function of the geometry. These quantities are therefore appropriate for the solid line curves on the graph, which correspond to the lowest value of incident pressure - low enough so that acoustic theory can be expected to apply. But the two quantities are quite artificial for the dashed-line curves, which correspond to higher values of incident pressure. The graph does, however, describe the results in a useful manner.

Let us consider first the solid lines - the low amplitude data. For angles of incidence near the normal, the results agree very well with acoustic theory. For incident angles greater than the critical angle of 26°, the results appear to be consistent with acoustic theory, although detailed calculations have not been made. The negative values of reflection factor correspond to the peak negative pressure contributions of the reflected pulses.

When the incident pressure is higher, as represented by the dashed curves, the reflection factor deviates from that for the acoustic case; the greater the incident pressure, the greater is the deviation. For incident angles smaller than critical, the deviation is toward smaller values of reflection factor; for incident angles greater than critical, the deviation is toward greater values of reflection factor. The data points offer no reliable indication of how to draw the empirical curves through the critical angle. As for the negative values of reflection factor, no effect of incident pressure is detectable through the scatter in the few usable data points; therefore only one curve was drawn through these points.

3. Ice Wave. Let us now consider briefly the arrival of what we designate as the ice wave. This is the same type of wave that has been variously called the ground wave, the head wave, and the precursor. A typical ice wave arrival is shown as the first event in record (a) of Figure 6. It has a slow rise and a low amplitude. The arrival time is determined from the ray path construction shown above this record. The path is the same as that used in geophysical sounding to determine the depths and sonic velocities of underground strata((l) and (m)). The ray approaches the ice at the critical angle; it refracts according to Snell's law, traveling along the interface at the

speed of sound in ice; and it emerges at many points, entering the water at the critical angle. The sound velocity in ice, incidentally, is between 10,000 and 11,000 feet per second, or just over twice the sound velocity in water.

4. Air-Reflected Wave. The air-reflected wave arrives over the path illustrated on the right side of Figure 6. Refraction occurs at the water-ice interface, and reflection occurs at the ice-air interface. Since the acoustic impedance of air is lower than that of ice, a negative reflection is expected from the ice-air interface.

The air-reflected wave appears as a cut-off of either the ice wave, as in record (a), or the reflected wave, as in record (b), depending upon the angle of incidence. The thicker the ice, the later is the arrival of the air-reflected wave.

5. Shear-Propagated Wave. In addition to the signals arriving over the four types of propagation path previously discussed, a fifth type of signal was observed on many of the pressure-time records. Arrival time calculations suggested that these signals correspond to propagation paths such as either of the two paths illustrated in Figure 7. These paths differ from the two paths in the previous figure, in that here the propagation velocity in ice is that of shear waves, only about 6,000 feet per second, rather than that of compressional waves. The angles of incidence and transmission are those that apply to this velocity. (See (m).)

The pressure-time record selected for illustration here is the one in which the peak pressure in the shear-propagated wave is greatest, relative to that in the direct wave.

C. PEAK PRESSURE CONTOURS

Figure 8 contains three space plots of peak pressure, one for each type of positive pulse involving the water-ice interface. R is the horizontal distance from the charge; D is the vertical distance from the image of the charge in the interface, as shown in the diagram. In the graphs both dimensions have been scaled to the cube root of the charge weight, W, so that data for all the charge weights could be plotted together.

These graphs indicate that for each type of pulse there is some region where its peak pressure contribution is greater than those of the other two types of pulse.

D. COMPLETE PRESSURE RECORDS

Some examples of complete pressure-time records will now be shown (Figure 9) to illustrate the relative pressures and arrival times of the various pulses, for a variety of geometries.

In record (a) the reflected wave is a positive pulse superposed on the tail of the direct wave, and both are cut off by the negative air-reflected wave.

In record (b) the ice wave and air-reflected wave arrive before the direct shock wave. The reflected pulse, which arrives later, consists of a small positive peak followed immediately by a large negative signal. The resultant absolute pressure at that time goes no lower than about zero, because natural water is unable to sustain appreciable tensions. The final arrival is the shear-propagated wave.

In record (c) both the reflected wave and the ice wave are superposed on a portion of the direct wave, and all three are cut off by the air-reflected wave.

In record (d) the peak pressure in the reflected wave is great enough and arrives early enough so that the resultant peak pressure is greater than that due to the direct wave alone.

Record (e), in which the time scale is greatly compressed, represents a long-range shallow-layer case. The horizontal distance from the charge to the gage was 600 feet, and the average water depth was about 50 feet. The first positive pulse is the direct shock wave; the following negative signal is probably the reflection from the ice; and the next negative signal is probably the reflection from the bottom of the lake. Subsequent signals represent multiple reflection paths. Each signal may be expected to be characterized by the cumulative phase changes it has undergone at all its reflections. (See (k).)

The data from Moonshine Lake, together with information on the appropriate characteristics of the various types of Arctic ice, can be used as a basis for predicting the pressure histories for a wide variety of configurations. These results may then be studied in an attempt to determine what modifications, if any, should be made in the estimates of damage ranges and weapon delivery ranges due to the presence of ice.

III. ICE BREAKING

Data from explosions tests beneath both lake ice and sea ice have been applied to the problem of breaking a clearing in thick ice by the use of an underwater explosion, in order to give a submarine quick access to the surface.

As a historical footnote, this method was first proposed in an article entitled "To the North Pole in a Submarine Boat with Dynamite to Blow Holes in the Ice". The article was written by the pioneer submarine designer, Simon Lake, in 1898.

The energy available for breaking ice by an underwater explosion includes not only the energy in the shock wave pulse, but also the energy associated with the subsequent bubble of gaseous explosion products. Normally, the gas bubble expands to its maximum size, and then alternately contracts and expands until its energy is dissipated, or until it migrates to the surface because of buoyancy, and vents. At the end of each contraction phase, the bubble emits a pressure pulse.

Figure 10 shows a sequence of photographs of the above-surface effects of an under-ice explosion. Typically, the shock wave pulse causes the ice layer to rise in the shape of a shallow dome, as in photograph (a). The effect of the bubble appears either before or after the dome begins to fall back, depending upon the depth of explosion. As the bubble reaches the surface, pieces of ice are thrown out, either mostly upward or mostly radially, depending upon the phase of the bubble motion at the time it vents. The resulting hole contains ice debris of variable concentration and size distribution.

Figure 11 is a graph of the resultant hole radius as a function of the charge depth, for the three charge sizes used at Moonshine Lake. For each charge size, there appears to be an optimum charge depth - that is, the charge depth yielding the largest hole.

The optimum charge depth, and the corresponding hole radius, are both approximately proportional to the cube root of the charge weight. This is not surprising, in view of the following two well-established scaling laws for geometrically similar configurations, one relating to the shock wave, and the other to the bubble. First, the distance at which a given value of peak shock wave pressure occurs is proportional to the cube root of the charge weight; and second, the maximum bubble radius expected in free water is approximately proportional to the cube root of the charge weight, for shallow charge depths.

The peculiar shapes of these three curves can be shown to be related to the size and the dynamic state of the bubble at the time it vents, as a function of the depth of explosion. This suggests that the bubble plays a more important role than the shock wave in determining the size of the hole.

This result could be quite useful in satisfying the operational requirements for a particular proposed ice-breaking application. The requirements are that the hole size be maximized, while the safe standoff distance of the submarine during the explosion be minimized, so that the submarine can find the hole quickly and reliably. The safe standoff distance is a function of the shock wave parameters of the explosion. If, on the other hand, the hole size is a function of the bubble parameters, we can improve the tactical usefulness of the device by choosing an explosive yielding relatively high bubble energy but relatively low shock wave energy. (See (n).)

In order to obtain further evidence of the role of the bubble in determining hole size, a laboratory experiment was conducted, in which one-gram charges of various compositions were fired at the optimum depth beneath a sheet of material simulating ice. Figure 12 shows two properties of the explosive, and the resultant hole radius, each as a function of the explosive mixture - specifically, as a function of the proportions of PETN and aluminum in the charge. The quantities in all three curves are expressed relative to their values for the reference charge, which contains no aluminum.

This graph demonstrates quite clearly that, at least for the ice simulant, the hole radius is approximately proportional to the bubble radius, rather than to the shock wave characteristics.

For sea ice tests we therefore recommended HBX-3, a standard explosive which has a relatively large ratio of bubble energy to shock wave energy, although not as extreme as the optimum condition on this graph.

Figure 13 compares the sea ice results (c) with Moonshine Lake. All dimensions have been drawn scaled to the free-water maximum bubble radius, in order to illustrate a test of the prediction that there is a constant ratio of the hole radius to the bubble radius. The proportionality factor of 2, which was found to apply to all three charge sizes at Moonshine Lake, is found not to apply to the two sea ice test series. The differences in the proportionality factor may possibly be attributed both to differences in scaled ice thickness, as a first glance at this graph might suggest, and to differences in the strength characteristics of sea ice (see (p)). Within each

test series, however, the variation in hole radius, as a function of charge size and charge depth, was consistent with the Moonshine Lake results.

This indicates that the Moonshine Lake results, together with only a limited amount of data for each of the various types of sea ice, as such data become available, can be used with reasonable confidence to predict hole formation for a wide range of charge sizes and ice conditions. Predictions based on existing data are now being used in studies relating to the design of submarine-launched ice destructors for use in various tactical situations.

REFERENCES

(a) J. H. Rosenbaum and H. G. Snay, "On the Oblique Reflection of Underwater Shock Waves from a Free Surface, I", NAVORD Report 2710, First Revision (1956), Unclassified.
(b) J. H. Rosenbaum, "On the Oblique Reflection of Underwater Shock Waves from a Free Surface, II", NAVORD Report 2855 (1953), Confidential.
(c) J. H. Rosenbaum, "On the Oblique Reflection of Underwater Shock Waves from a Free Surface, III", NAVORD Report 2943 (1953), Confidential.
(d) E. A. Christian and J. H. Rosenbaum, "On the Oblique Reflection of Underwater Shock Waves from a Free Surface, IV. Charges at the Surface", NAVORD Report 3680 (1954), Confidential.
(e) T. B. Heathcote, "On the Oblique Reflection of Underwater Shock Waves from a Free Surface, V. Data from Small Charges", NAVORD Report 6738 (1960), Confidential.
(f) J. H. Rosenbaum, "Shock Wave Propagation in Shallow Water, I", NAVORD Report 4353 (1956), Unclassified.
(g) J. H. Rosenbaum, "Shock Wave Propagation in Shallow Water, II", NAVORD Report 4354 (1956), Unclassified.
(h) C. R. Niffenegger and T. B. Heathcote, "Shock Wave Propagation in Shallow Water. III. Pressure, Durations, Impulses, and Craters from 100-lb TNT Charges", NAVORD Report 6077 (1958), Confidential.
(i) C. L. Pekeris, "Theory of Propagation of Explosive Sound in Shallow Water", Geological Society of America, Memoir 27 (1948), Unclassified.
(j) R. H. Cole, "Underwater Explosions", Princeton University Press, Princeton, N. J. (1948), Unclassified.
(k) A. B. Arons and D. R. Yennie, "Phase Distortion of Acoustic Pulses Obliquely Reflected from a Medium of Higher Sound Velocity", Journal of the Acoustical Society of America 22, 231-237 (1950), Unclassified.
(l) C. Herring, "The Physics of Sound in the Sea", Summary Technical Report of Division 6, NDRC, Vol. 8, Sec. 9.4, (1946), Unclassified.
(m) M. Muskat, "The Theory of Refraction Shooting", Journal of Applied Physics 4, 14-28 (1933), Unclassified.
(n) E. A. Christian, "The Contribution of Aluminum to the Effectiveness of an Explosion. I. Underwater Performance of One-Pound Charges", NAVORD Report 3760 (1954), Confidential.
(o) D. M. Leslie and C. A. Nelson, "Explosion Tests Under Thick Polar Ice", NOLTR 61-146 (1961), Confidential; contains additional references to unpublished reports on explosive ice-breaking.
(p) "Arctic Sea Ice", National Academy of Sciences - National Research Council Publication 598 (1958), Unclassified.

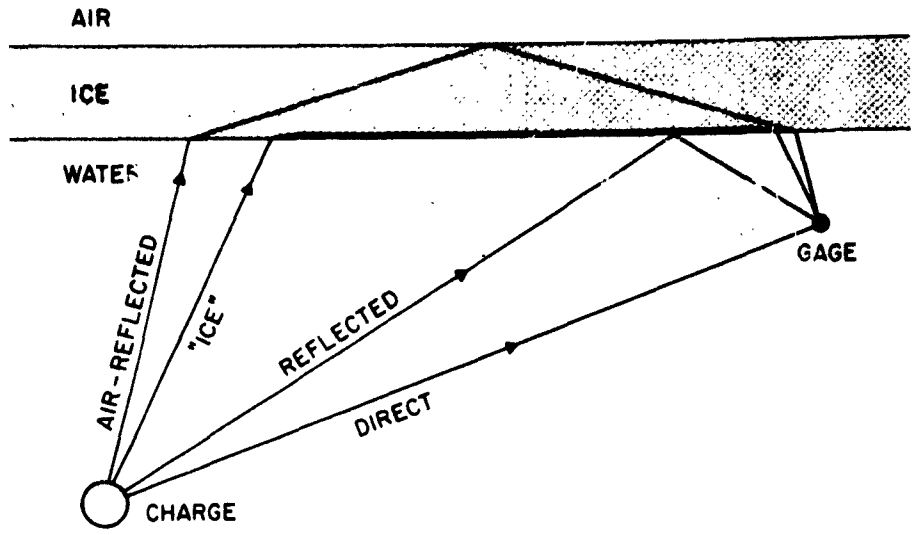

FIG. 1 SHOCK WAVE PROPAGATION PATHS

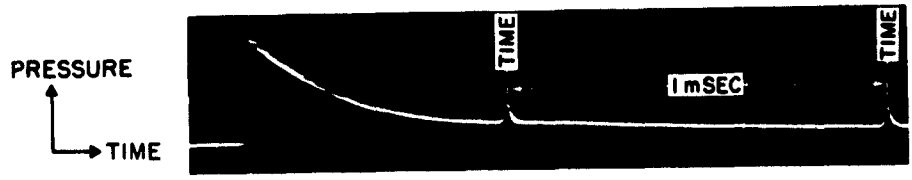

FIG. 2 DIRECT SHOCK WAVE

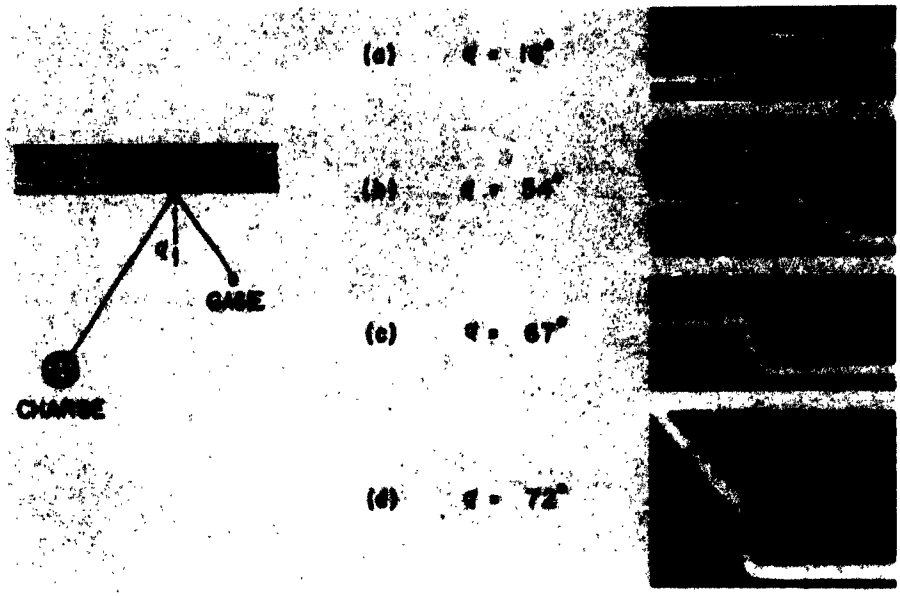

FIG. 3 REFLECTED WAVE VS ANGLE OF INCIDENCE

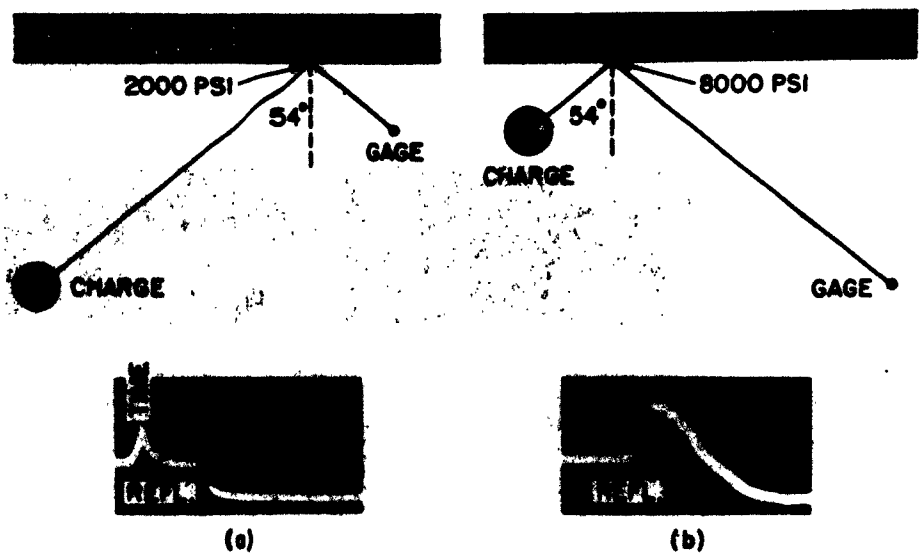

FIG. 4 REFLECTED WAVE VS INCIDENT PRESSURE

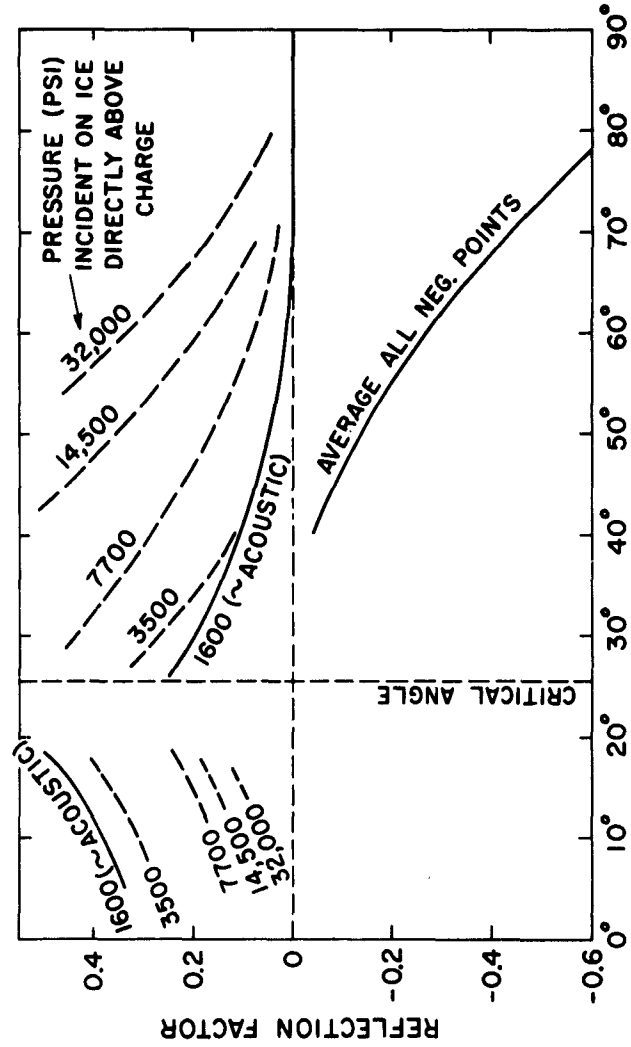

FIG. 5 REFLECTION FACTOR VS ANGLE OF INCIDENCE

FIG. 6 ICE WAVE AND AIR-REFLECTED WAVE

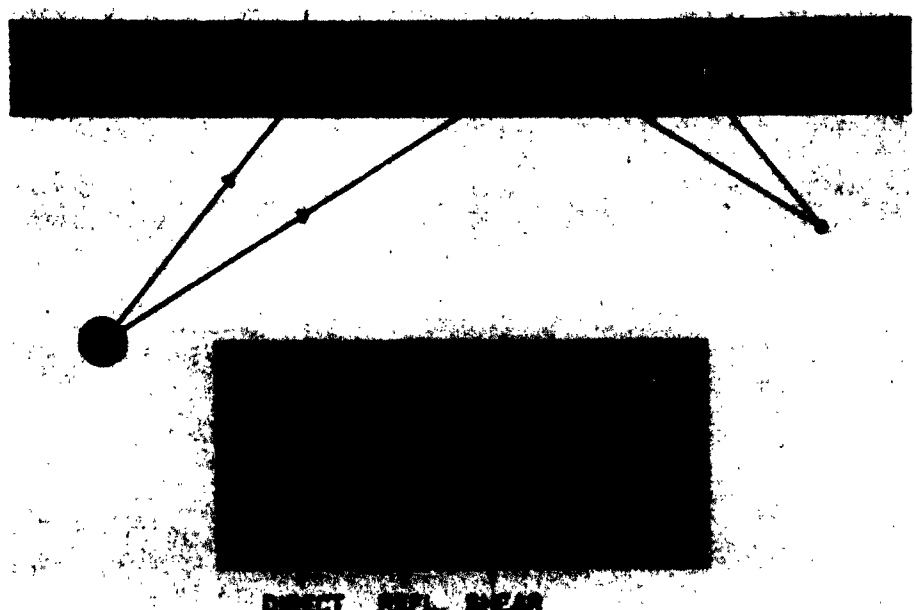

FIG. 7 SHEAR-PROPAGATED WAVE

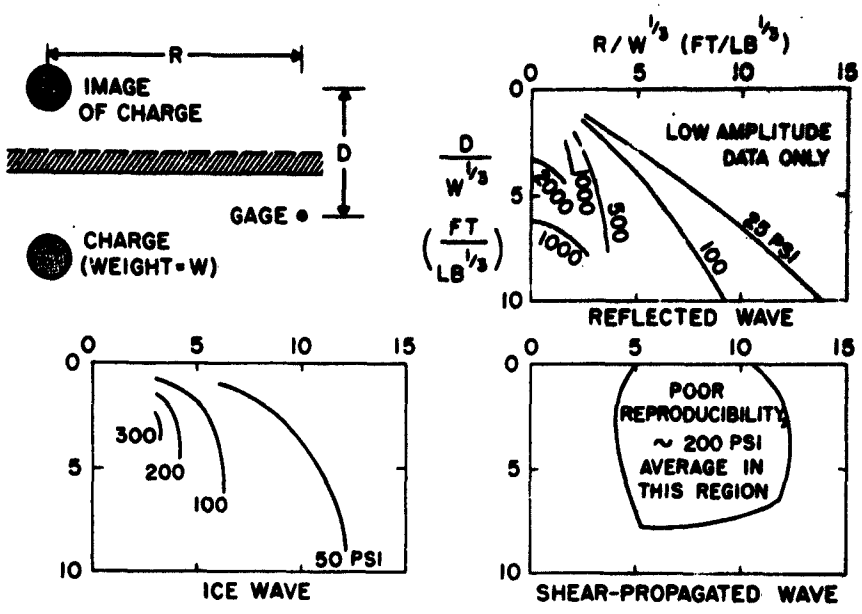

FIG. 8 PEAK PRESSURE CONTOURS

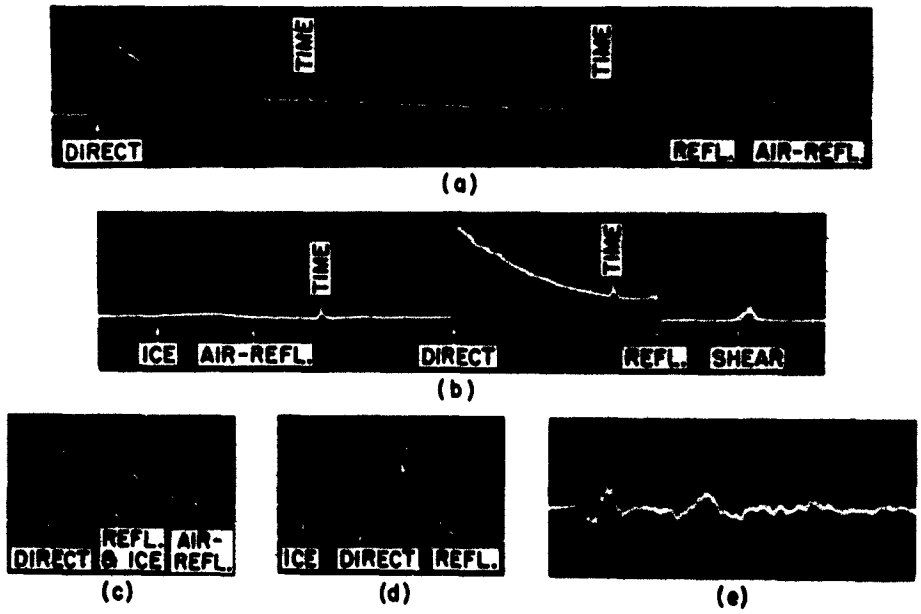

FIG. 9 COMPLETE PRESSURE-TIME RECORDS

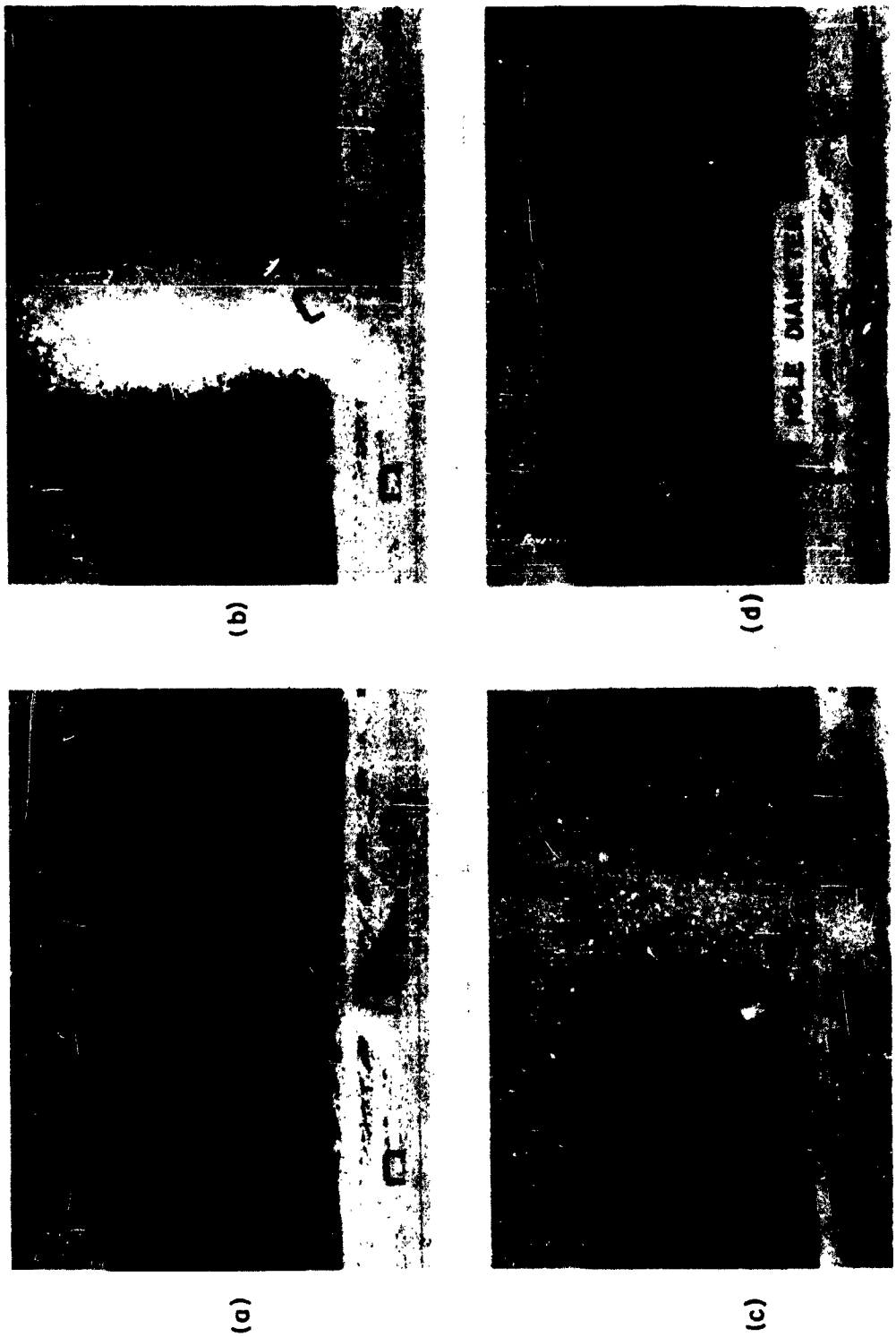

FIG. 10 PHOTOGRAPHIC SEQUENCE: UNDER-ICE EXPLOSION

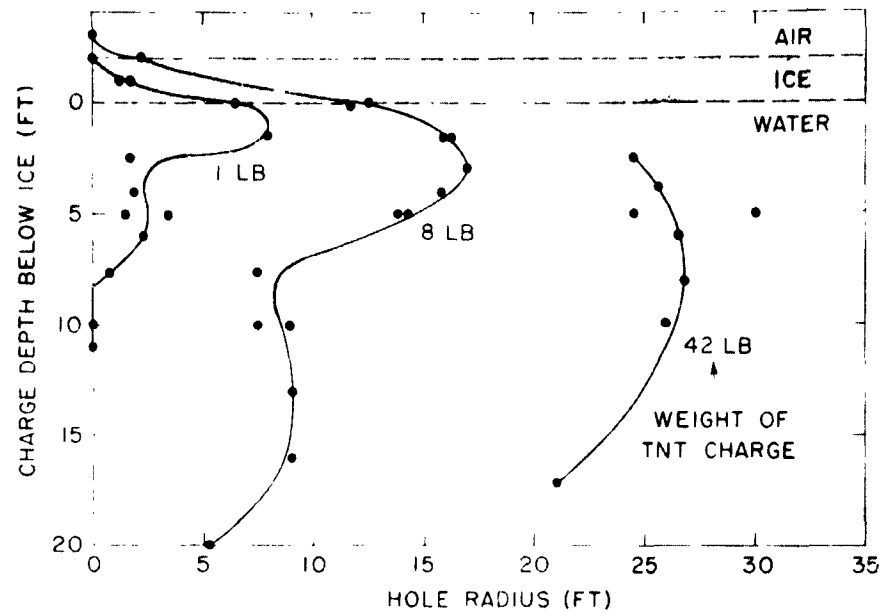

FIG. 11 HOLE RADIUS IN ICE VS CHARGE DEPTH

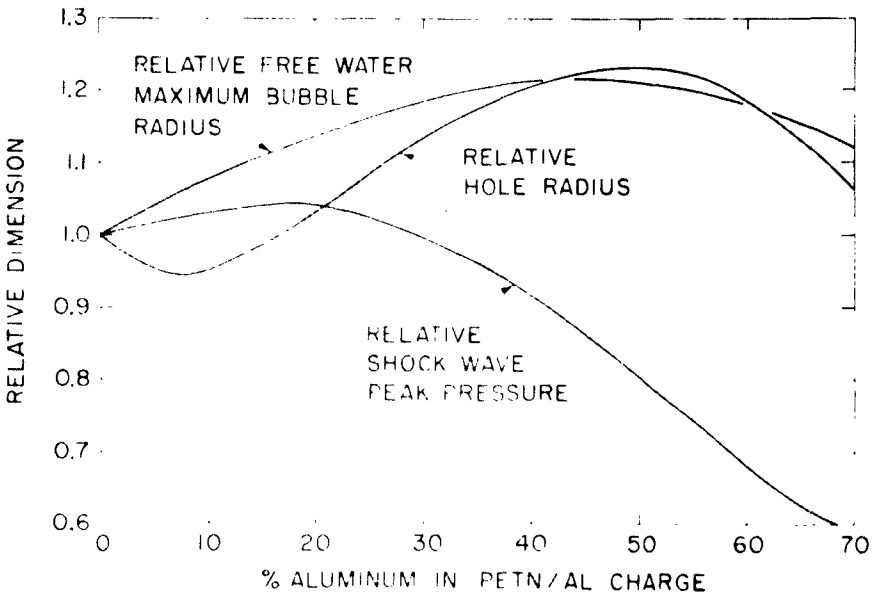

FIG. 12 HOLE RADIUS FOR VARIOUS EXPLOSIVE MIXTURES

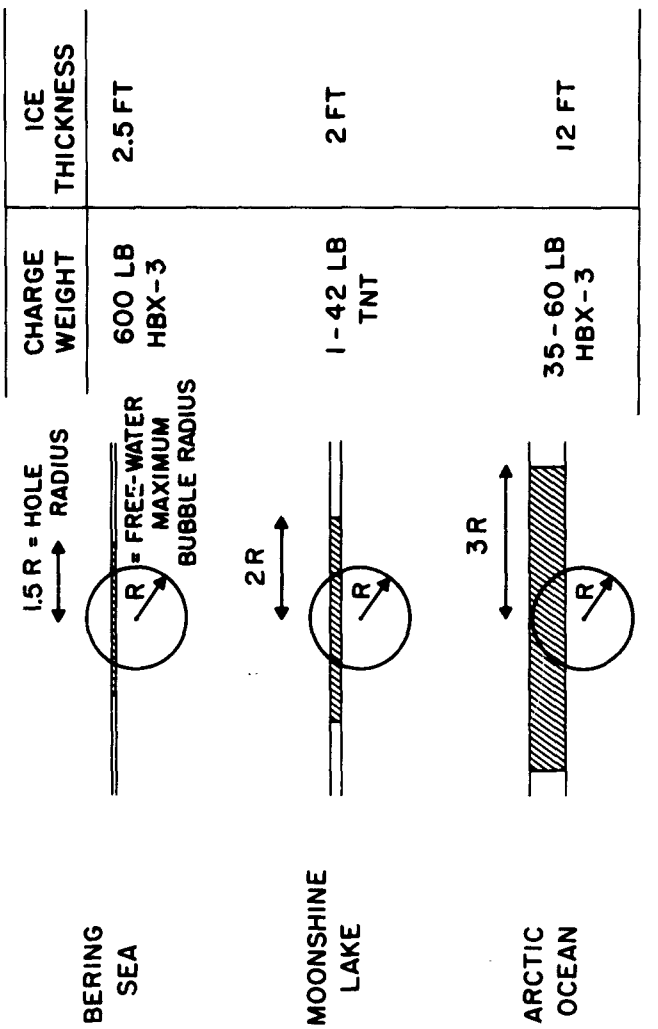

FIG. 13 COMPARISON OF THREE TEST SERIES

DISTRIBUTION

	Copies
Chief, Bureau of Naval Weapons, Attn: Tech Lib DIS-3	2
Attn: RUME-3	1
Attn: RRRE-5	2
Attn: RUME-231	1
Chief of Naval Operations, Attn: OP-715	1
Chief of Naval Research, Attn: Code 466	1
Attn: Code 418	1
Attn: Code 429	1
Attn: Geographic Branch (Dr. M. E. Britton)	1
Chief, Bureau of Ships, Attn: Code 423	2
Chief, Bureau of Yards and Docks	1
Commanding Officer and Director, U. S. Naval Radiological Defense Laboratory, San Francisco 24, California	
Attn: Code 911	1
Attn: Code 934	1
Attn: Code 222	1
Commanding Officer, Naval Propellant Plant, Indian Head, Maryland	1
Commander, Naval Weapons Laboratory, Dahlgren, Virginia	
Attn: Experimental Officer	1
Commander, Naval Ordnance Test Station, China Lake, California, Attn: Technical Library	1
Commander, Naval Ordnance Test Station, Pasadena, California	1
Director, Naval Research Laboratory, Washington, D. C.	2
Commanding Officer and Director, David Taylor Model Basin, Washington 7, D. C.	2
Commanding Officer and Director, David Taylor Model Basin, Underwater Explosions Research Division, Portsmouth, Virginia (Code 780)	1
Superintendent, U. S. Naval Postgraduate School, Monterey, California	1
Director, U. S. Navy Electronics Laboratory, San Diego, California	1
Attn: Dr. W. K. Lyon	1
Commanding Officer, U. S. Naval Underwater Ordnance Station, Newport, Rhode Island	1

DISTRIBUTION (Cont'd)	Copies
Commander, U. S. Naval Weapons Station, Yorktown, Va. Attn: Research and Development Division	1
Commanding Officer, Naval Torpedo Station, Keyport, Washington	1
Commanding Officer and Director, U. S. Navy Underwater Sound Laboratory, New London, Conn.	1
Attn: R. J. Hecht	1
Commanding Officer, U. S. Naval Air Development Center, Johnsville, Pennsylvania	1
Commanding Officer, U. S. Naval Ammunition Depot, Navy Number 66, Fleet Post Office, San Francisco, California Attn: Quality Evaluation Laboratory	1
The Hydrographer, Naval Hydrographic Office, Suitland, Md.	1
Attn: W. Wittman	1
Commanding Officer, U. S. Navy Mine Defense Laboratory, Panama City, Florida	1
Commanding Officer and Director, Naval Civil Engineering Laboratory, Port Hueneme, California	1
Commanding Officer, U. S. Naval Weapons Evaluation Facility, Kirtland Air Force Base, Albuquerque, New Mexico	1
Chief of Research and Development, Department of the Army, Washington, D. C.	1
Chief of Ordnance, Department of the Army, Washington 25, D. C.	2
Chief of Engineers, Department of the Army, Washington 25, D. C. Attn: ENGNB	2
Attn: ENGEB	1
Director, Waterways Experiment Station, Vicksburg, Mississippi Attn: F. R. Brown	1
Attn: L. Ingram	1
Commanding General, Ballistic Research Laboratories, Aberdeen, Maryland	1
Commanding Officer, Picatinny Arsenal, Dover, New Jersey	1
Commanding Officer, Engineer Research and Development Laboratory, Fort Belvoir, Va. Attn: Chief, Tech Support Branch	1

DISTRIBUTION (Cont'd)	Copies
Commanding Officer, USA Signal R and D Laboratory, Fort Monmouth, New Jersey, Attn: Tech. Documents Center	1
Director of Research and Development, Headquarters, U. S. Air Force, Washington 25, D. C.	1
Commander, Ooama, Attn: Air Force Ammunition Services Office, Hill Air Force Base, Utah	1
Headquarters, Air Proving Ground Center, U. S. Air Force, ARDC, Eglin Air Force Base, Florida Attn: PGTRI, Tech. Lib.	1
Commander, Air Force Logistics Command, Wright-Patterson Air Force Base, Dayton, Ohio	1
Aeronautical System Division, Wright-Patterson Air Force Base, Dayton, Ohio	1
Commander, Air Force Special Weapons Center, Kirtland Air Force Base, Albuquerque, New Mexico, Attn: Tech Lib	1
Director, Defense Research and Engineering, Washington 25, D. C. Attn: Tech Lib	1
Director, Applied Physics Laboratory, Johns Hopkins University, Silver Spring, Maryland	1
Chief, Defense Atomic Support Agency, Washington 25, D.C.	3
Director, Applied Physics Laboratory, University of Washington, Seattle, Washington	1
Director, Operations Research Office, Johns Hopkins University, 6935 Arlington Road, Bethesda, Maryland Attn: Document Control Office Washington 14, D. C.	1
Director, Ordnance Research Laboratory, Pennsylvania State University, University Park, Pennsylvania	1
Director, Woods Hole Oceanographic Institution, Woods Hole, Mass.	1
Director, Scripps Institute of Oceanography, La Jolla, California	1
Columbia University, Hudson Laboratories, 145 Palisade Street, Dobbs Ferry, N. Y.	1
Director, Lawrence Radiation Laboratory, Livermore, Calif.	1
Director, Los Alamos Scientific Laboratory, Los Alamos, New Mexico, Attn: D. P. MacDougall	2

DISTRIBUTION (Cont'd)	Copies
Director, National Bureau of Standards, Washington, D. C. Attn: Security Officer	1
Administrator, NASA, 1512 H Street, N. W., Washington, D. C.	1
Sandia Corporation, Sandia Base, Albuquerque, New Mexico Attn: Classified Document Division	1
Armed Services Technical Information Agency, Arlington Hall Station, Arlington 12, Virginia, Attn: TIPDR	10
Under Sea Warfare Group, U. S. Naval Ordnance Laboratory, White Oak, Silver Spring, Maryland Attn: Dr. Raff	1
Amherst College, Amherst, Mass. Attn: Dr. Arnold Arons Physics Dept	1
New York University, University Heights, New York 53, New York Attn: Dr. G. E. Hudson, Dept of PHysics	1
Michigan State University, East Lansing, Michigan c/o Mr. Gerald Knapp, Security Officer, Administration Bldg., Attn: Dr. T. Triffet, Dept. of Applied Mech.	1
Harvey Mudd College, Claremont, California Via: ONR Branch Office, Pasadena Calif Attn: Dr. A. B. Focke, Dept of Physics	1
Columbia University, New York 27, New York Attn: Dr. H. H. Bleich, Dept of Civil Engr and Engr. Mech.	1
University of Alaska, Geophysical Institute, College, Alaska Attn: Dr. C. T. Elvey	1
University of New Hampshire, Durham, New Hampshire Attn: Dr. H. H. Hall (Contract N60921-7015)	1
Arctic Research Laboratory, Point Barrow, Alaska Attn: Max Brewer	1
U. S. Army Cold Regions Research and Engineering Laboratory, Post Office Box 282, Hanover, N. H.	1

CATALOGING INFORMATION FOR LIBRARY USE

BIBLIOGRAPHIC INFORMATION

	DESCRIPTORS	CODES		DESCRIPTORS	CODES
SOURCE	NOL technical report	NOLTR	SECURITY CLASSIFICATION AND CODE COUNT	Confidential - 18	CØ18
REPORT NUMBER	62-96	62ØØ96	CIRCULATION LIMITATION		
REPORT DATE	1 June 1962	Ø662	CIRCULATION LIMITATION OR BIBLIOGRAPHIC		
			BIBLIOGRAPHIC (SUPPL., VOL., ETC.)		

SUBJECT ANALYSIS OF REPORT

DESCRIPTORS	CODES	DESCRIPTORS	CODES	DESCRIPTORS	CODES
Ice	ICEA	Pressure	PRES		
Underwater	UNDE	High	HIGH		
Explosions	EXPS	Bubble	BUBB		
Ice (Effects)	ICEAE	Energy	ENER		
Nuclear	NUCL	Propagation	PROO		
Damage	DAMA	Arctic Ocean	ARTI		
Range	RANG				
Destructor (Design)	DESUD				
Submarines	SUBM				
Surfacing	SRFC				
Shock	SHOC				
Wave	WAVE				